



# Ordered mesoporous tungsten carbide/carbon composites promoted Pt catalyst with high activity and stability for methanol electrooxidation

Kun Wang<sup>a</sup>, Yi Wang<sup>b</sup>, Zhenxing Liang<sup>c</sup>, Yeru Liang<sup>b</sup>, Dingcai Wu<sup>b</sup>, Shuqin Song<sup>a,\*</sup>, Panagiotis Tsakaras<sup>d,\*</sup>

<sup>a</sup> State Key Laboratory of Optoelectronic Materials and Technologies/The Key Lab of Low-carbon Chemistry & Energy Conservation of Guangdong Province, School of Physics and Engineering, Sun Yat-sen University, Guangzhou 510275, China

<sup>b</sup> School of Chemistry and Chemical Engineering, Sun Yat-sen University, Guangzhou 510275, China

<sup>c</sup> Key Lab for Fuel Cell Technology of Guangdong Province, School of Chemistry and Chemical Engineering, South China University of Technology, Guangzhou 510641, China

<sup>d</sup> Department of Mechanical Engineering, School of Engineering, University of Thessaly, Pedion Areos, Athens 38834, Greece

## ARTICLE INFO

### Article history:

Received 4 July 2013

Received in revised form

13 September 2013

Accepted 16 September 2013

Available online 25 September 2013

### Keywords:

Methanol electrooxidation

Ordered mesoporous carbon (OMC)

Tungsten carbide

Pt@WC/OMC

## ABSTRACT

The current anode materials used for direct methanol fuel cells (DMFCs) are expensive and not sufficiently durable for commercial development. One of the major challenges lies in the development of an inexpensive, efficient and stable anode catalyst. In the present manuscript ordered mesoporous tungsten carbide/carbon composites promoted Pt (Pt@WC/OMC) catalyst with high activity and stability for methanol electrooxidation is reported. WC/OMC nanomaterials have been synthesized by combining the hydrothermal reaction and the hard-template method and they have been platinized by a pulse microwave assisted polyol technique. The combination of high surface area, ordered mesopores, the synergistic effect and CO-tolerant ability of WC and well dispersed Pt nanoparticles provide Pt@WC/OMC with high activity, desirable stability, and CO-tolerance toward methanol electrooxidation. Compared with the commercial PtRu@C (40 wt.% Pt, 20 wt.% Ru) catalyst, Pt@WC/OMC demonstrates longer stability as well as higher specific mass activity for methanol electrooxidation by a factor of 1.1 (per mg Pt) and 1.7 (per mg noble metal). Experimental results have proved that Pt@WC/OMC is a promising anode catalyst for DMFCs applications.

© 2013 Elsevier B.V. All rights reserved.

## 1. Introduction

Direct methanol fuel cells (DMFCs) have been attractive as a new, clean alternative power source for portable electronic devices. This is due to their high energy density, near room temperature operation, longer-lasting power compared with a rechargeable battery, instantaneous recharging by simply replacing the disposable fuel cartridge, non-toxic disposal, and light weight [1,2]. Currently, there still exist many challenges for commercializing DMFCs, including the undesirable activity, kinetics, durability and high cost of Pt-based catalysts. Consequently, to break through these major bottlenecks, it is vital to identify and develop highly efficient, durable and inexpensive catalysts. Today, PtRu based electrocatalysts are the most widely adopted and well recognized as the best

anode materials in DMFCs due to their reliable methanol electrooxidation performance. However, their low specific mass activity and thereby their high cost [3], high sensitivity to CO [4], and instability [5–9] are their main drawbacks that make PtRu-based electrocatalysts unsatisfactory for practical DMFCs applications. Moreover, Ru is susceptible to leach out from PtRu catalysts [10–14], which not only continuously deteriorates the anode activity [11], but also leads to about 40–200 mV decrease in the cell performance caused by “Ru crossover” [13]. The dissolved Ru at the anode can permeate through the electrolyte membrane to the cathode and can be re-deposited on the cathode catalyst [12]. Hence, new type Ru-free, more efficient and more stable electrocatalysts for methanol electrooxidation are still highly desirable.

Tungsten carbides have been widely used in machines due to their superior hardness, high melting point, good resistance to fracture, wear, oxidation and corrosion [15,16]. Recently, tungsten carbides have attracted much attention because of their similar catalytic activity to that of Pt group metals [17,18], possessing desirable stability in both acidic and alkaline solutions [19–25], as well as high tolerance to both CO and H<sub>2</sub>S poison [26,27]. Moreover,

\* Corresponding authors.

E-mail addresses: [stssq@mail.sysu.edu.cn](mailto:stssq@mail.sysu.edu.cn) (S. Song), [tsiak@uth.gr](mailto:tsiak@uth.gr) (P. Tsakaras).

<sup>1</sup> Tel: +86 20 84113253; fax: +86 20 84113253.

<sup>2</sup> Tel.: +30 24210 74065; fax: +30 24210 74050.

synergistic effects on Pt's activity to methanol electrooxidation have also been reported [28–31]. Among tungsten carbides, WC is found to be more stable than  $W_2C$  in an electrochemical environment.  $W_2C$  can be immediately oxidized to  $W_xO_y$  species, while WC is stable at the anode potential below 0.6 V (vs. NHE) [22,23].

Since the discovery of ordered mesoporous solids of the MCM-41 type and related materials in the early 1990s [32], ordered mesoporous materials have become a research focus and have been widely used in catalysis. This is due to their relatively large pores which facilitate mass transfer and the very high surface area which allows a high concentration of active sites per mass of material [33]. Through soft-template and hard template method, various self-supported ordered mesoporous materials with variable composites have been synthesized. Unfortunately, these two methods are difficult for the preparation of ordered mesoporous self-supported metal carbides. This is due to the lack of proper precursors for so-gel process in soft-template method and very possible collapse of the mesoporous regularity in the conversion of metal precursor to carbide in the hard-template method [34]. Until now, to our best knowledge, there is no report about the synthesis of self-supported ordered mesoporous transition carbides. Considering also the inherent property of high density of WC and the necessary high temperature synthesis conditions for WC formation, ordered mesoporous WC is difficult to be synthesized. One of the feasible ways is to evenly load WC on carbon materials or to functionalize carbon with WC in order to obtain WC/carbon composites, which have exhibited excellent performance in DMFCs [28–31].

In the present work, ordered mesoporous tungsten carbide/carbon (WC/OMC) composite was synthesized by combining the hydrothermal reaction and hard template method. In this process, ammonium metatungstate (AMT) was used as tungsten precursor, glucose as the carbon source and the ordered mesoporous silica (SBA-15) as the hard template. Thereafter, Pt nanoparticles were deposited on the as-prepared OMC/WC, leading to Pt@WC/OMC electrocatalyst for methanol electrooxidation, exhibiting high activity, desirable CO tolerance and good stability.

## 2. Experimental

### 2.1. Synthesis of WC/OMC and ordered mesoporous carbon (OMC)

WC/OMC sample was prepared by combining the hydrothermal reaction and the hard template method with ammonium metatungstate (AMT) as tungsten precursor, glucose as the carbon source and the ordered mesoporous silica (SBA-15) as the hard template, respectively. The preparation procedure is shown in Fig. 1 and described in details as follows. In a flask, 0.736 g AMT and 1.982 g glucose were dissolved in distilled water and mixed with 1.000 g SBA-15 under stirring for several hours. Subsequently, the above mixture was transferred into an autoclave for reaction at 180 °C for 12 h. After reaction, the solution mixture was poured into a disk and then dried at 90 °C for 12 h in order to remove the solvent. Then the as-prepared product was carbonized at 900 °C for 3 h in  $N_2$  and  $H_2$  mixed atmosphere ( $V_{N_2}/V_{H_2} = 3/1$ ). The heating rate was controlled to be 5 °C min<sup>-1</sup>. The resulting sample was washed in HF solution (40 wt.%) under stirring to remove SBA-15 hard template, and then filtered, washed, and dried at 90 °C for 12 h in a vacuum oven. The final product was defined as WC/OMC.

For comparison, the ordered mesoporous carbon (OMC) was also prepared by the hard template method [35]. The SBA-15 (1.000 g) was added into the solution obtained by dissolving 1.250 g sucrose and 0.150 g  $H_2SO_4$  in 5.0 mL  $H_2O$ . The mixture was reacted at 100 °C for 6 h and then at 160 °C for another 6 h. After the first drying composites were grinded, the second heating process was

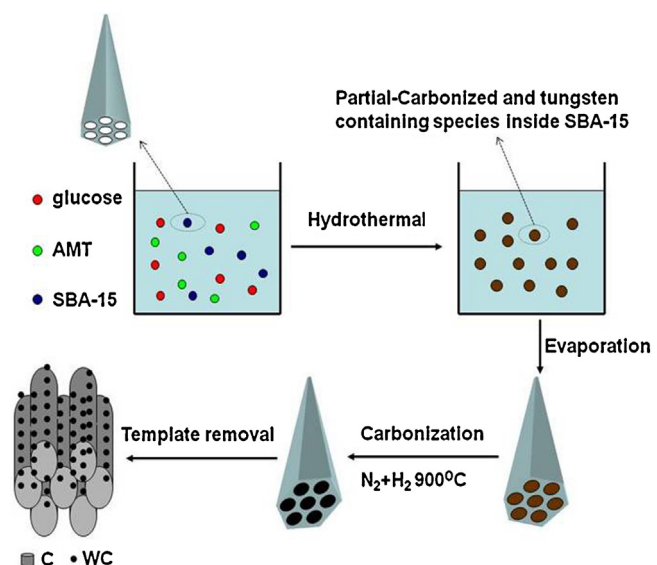


**Fig. 1.** Synthetic process of ordered mesoporous tungsten carbide/carbon composites with SBA-15 as a hard-template, ammonium metatungstate salt (AMT) as the tungsten precursor, and glucose as the carbon source, respectively, by combining a hydrothermal reaction and a hard template method.

performed with additional precursor solution (0.800 g sucrose and 0.080 g  $H_2SO_4$  in 5.0 mL  $H_2O$ ). After that, the sample was heated to 900 °C at a heating rate of 5 °C min<sup>-1</sup>, and kept at 900 °C for 3 h in  $N_2$  atmosphere. Finally, the carbon/SBA-15 composites were washed using HF solution (40 wt.%) for removing SBA-15 to obtain OMC.

### 2.2. Preparation of electrocatalysts

The Pt@WC/OMC and Pt@OMC catalysts with a Pt loading of 20 wt.% were prepared by a pulse-microwave assisted polyol method [36,37]. The as-prepared WC/OMC or OMC as the supporting materials was well mixed with ethylene glycol (EG) in an ultrasonic bath and then an appropriate amount of  $H_2PtCl_6 \cdot 6H_2O$  dissolved in EG was added into the mixture. After the pH value of the above mixture was adjusted to more than 10 by the dropwise addition of 1.0 mol L<sup>-1</sup> NaOH/EG solution, a well-dispersed slurry was obtained with magnetic stirring for another 1 h. Thereafter, the slurry was microwave-heated in the pulse form of 10 s-ON/10 s-OFF for several times. After reaction, 1.0 mol L<sup>-1</sup> HCl solution was added to accelerate the deposition process. Finally, the resulting sample was filtered, washed with copious hot water ( $\geq 80$  °C) until no chloride anion was detected by 1.0 mol L<sup>-1</sup>  $AgNO_3$  solution in the filtrate and then dried at 90 °C overnight in a vacuum oven.

### 2.3. Characterization of electrocatalysts

#### 2.3.1. Physico-chemical characterization

The low-angle and wide-angle X-ray diffraction (XRD) patterns were recorded on a D-MAX 2200 VPC diffractometer using  $Cu K\alpha$  radiation (30 kV, 30 mA).  $N_2$  adsorption measurements were carried out using a Micromeritics ASAP 2010 analyzer at 77 K. The BET surface area ( $S_{BET}$ ) and the mesopore volume ( $V_{mes}$ ) were determined by BET theory and Barrett–Joyner–Halenda (BJH) method, respectively. The transmission electron microscopy (TEM) investigations were performed on a JEOL TEM-2010(HR) operating at 120 kV. Scanning electron microscopy (SEM) and element mapping were performed using Quatnta 400F thermal field emission environmental SEM.

### 2.3.2. Electrochemical characterization

All the electrochemical measurements were conducted on an AUT84480 instrument in a three-electrode cell with a saturated calomel electrode (SCE) and a Pt foil as the reference and counter electrode, respectively. The thin catalyst film was prepared onto the glassy carbon disk surface with a diameter of 0.5 cm. Typically, a mixture containing 10.0 mg electrocatalyst, 0.9 mL ethanol and 0.1 mL Nafion solution (5 wt.%, density: 0.874 g mL<sup>-1</sup> @ 25 °C, DuPont, USA) was ultrasonicated for 10 min and then stirred to obtain a well-dispersed ink. The catalyst ink (10 µL) was then quantitatively transferred onto the surface of the glassy carbon electrode and dried under infrared lamp to obtain a catalyst thin film. The Pt loading was maintained to be 101.9 µg Pt cm<sup>-2</sup>. It should be noted that all the potential was referred to the SCE without specification.

**2.3.2.1. Methanol activity evaluation.** For the electrocatalytic activity evaluation, the electrochemical tests were performed in 0.5 mol L<sup>-1</sup> H<sub>2</sub>SO<sub>4</sub> + 1.0 mol L<sup>-1</sup> CH<sub>3</sub>OH by cyclic voltammetry (CV). Before each experiment, the electrolyte solution was bubbled with high-purity N<sub>2</sub> for 30 min to remove the dissolved oxygen inside.

**2.3.2.2. CO stripping voltammetry.** In order to check the CO-tolerance of the as-prepared catalysts, CO-stripping voltammetry was adopted. CO was adsorbed onto the investigated catalysts by supplying pure CO at a flow rate of 40 mL min<sup>-1</sup> for 15 min, while keeping the working electrode potential at -0.15 V. The gas was then switched to high-purity Ar and kept for 30 min at a flow rate of 40 mL min<sup>-1</sup>, with the potential still held at -0.15 V, to remove any CO from the solution phase. The potential was scanned from the adsorption potential to 1.0 V at 20 mV s<sup>-1</sup>, to record the CO stripping voltammograms.

**2.3.2.3. Stability tests.** The long-term stability of the catalysts was tested by a continuous 1000 potential cycling at 50 mV s<sup>-1</sup> between -0.242 and 0.600 V in a 0.5 mol L<sup>-1</sup> H<sub>2</sub>SO<sub>4</sub> + 1.0 mol L<sup>-1</sup> CH<sub>3</sub>OH aqueous solution.

## 3. Results and discussion

The XRD patterns of the as-prepared WC/OMC composites in Fig. 2 show that the composition and structure of the products heavily depends on the synthetic conditions. With increasing the molar ratio of AMT to glucose from 0.026 to 0.039, the main phase is transferred from W<sub>2</sub>C and W to W<sub>2</sub>C and WC, which can be clearly seen from the XRD patterns of the samples before HF treatment (Fig. 2A). At the same molar ratio of AMT to glucose and the same reaction time, the increased temperature is beneficial for the formation of WC phase. After HF treatment for hard template removal, W<sub>2</sub>C and W phase disappears from the sample, indicating that W<sub>2</sub>C and W can be dissolved by HF solution and thus pure phase WC is easily obtained on the ordered mesoporous carbon. WC is more stable than W<sub>2</sub>C in acid media [22–25]. Chen's group demonstrated that WC was stable at anode potential below 0.6 V (vs. NHE) whereas W<sub>2</sub>C did not have a stable region, being oxidized to W<sub>x</sub>O<sub>y</sub> species immediately when exposed to air or in an electrochemical environment [22]. Accordingly, the pure phase WC is more desirable and feasible for fuel cell applications. Based on the above results and on the premise of making comprehensive consideration of structure, composition, size of WC and the cost of the synthesis procedure, the optimal AMT/glucose molar ratio of 0.039 and the reaction temperature of 900 °C was determined and adopted to prepare WC/OMC for further investigation. The WC/OMC obtained at the optimized synthesis conditions shows an ordered mesoporous structure (Figs. 3–5). From the low-angle XRD patterns of OMC and WC/OMC (Fig. 3), it can be distinguished that OMC exhibits an intense diffraction peak (10) and two resolved peaks

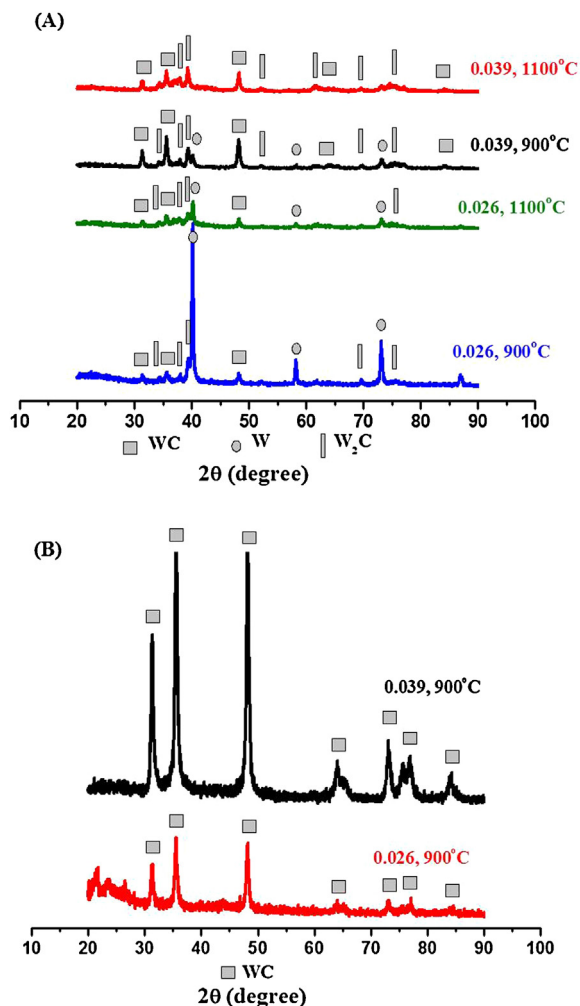


**Fig. 2.** XRD patterns of WC/OMC samples synthesized before (A) and after (B) HF treatment with different molar ratios of AMT to glucose and at different heat treatment temperatures.

(11) and (20), demonstrating the formation of a highly ordered 2D hexagonal mesostructure [35,38], which can be further verified by the parallel arranged channels observed from the TEM image of OMC (Figs. 4 A and B). When AMT was introduced as the tungsten precursor, the obtained WC/OMC has a lower order degree,

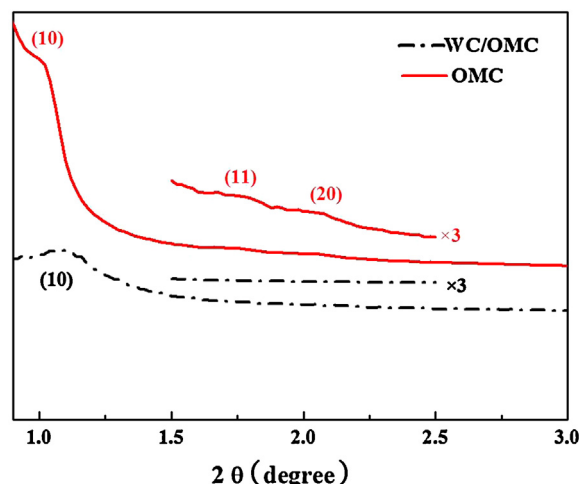


**Fig. 3.** Low-angle XRD patterns of OMC and WC/OMC samples.

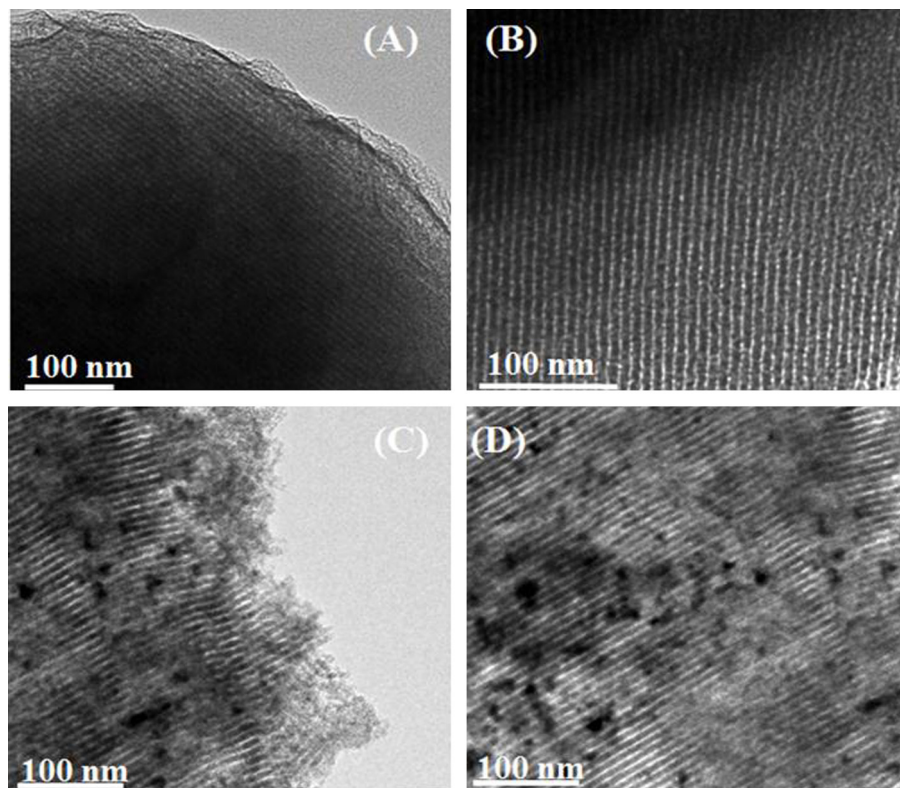


Fig. 4. TEM images of OMC ((A) and (B)) and WC/OMC ((C) and (D)).

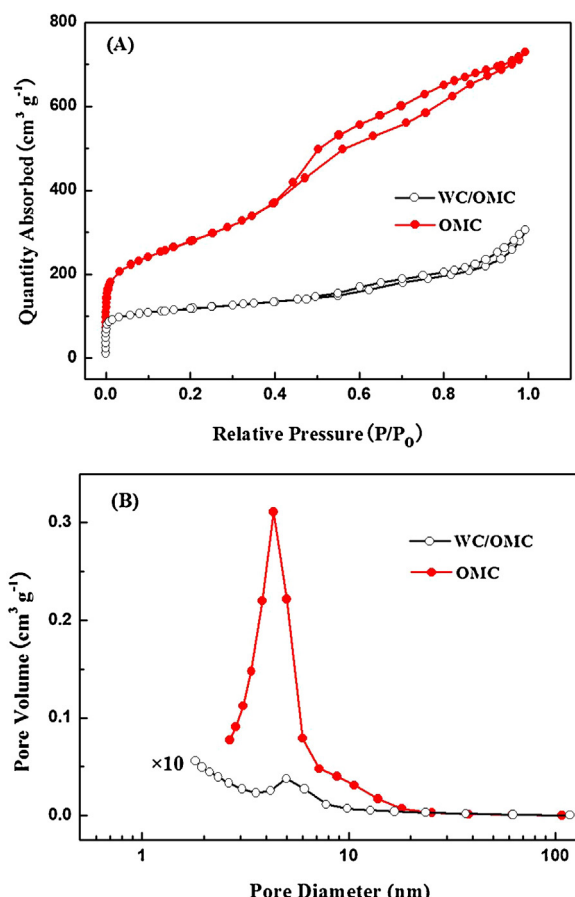
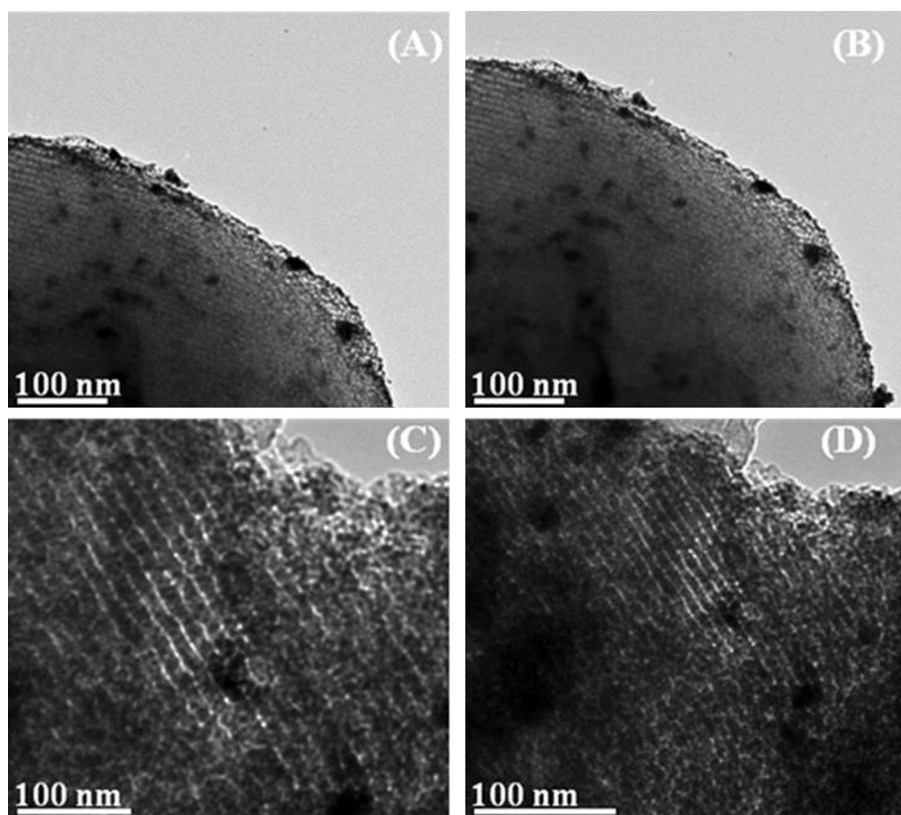


Fig. 5.  $N_2$  adsorption–desorption isotherms of OMC and WC/OMC samples (A) and their BJH pore size distributions (B).

which can be judged from the weaken strength of the diffraction peak (10) and the disappearance of the diffraction peaks (11) and (20) in Fig. 3. On the other hand, from TEM image of WC/OMC in Figs. 4 C and D, it is obvious that the ordered structure is still maintained. Clearly, the addition of AMT has some effect on the order degree of OMC, but does not hinder to form an ordered 2D hexagonal mesostructure, which gives us the practicability to synthesize WC/OMC composites.

In order to investigate the pore structure of OMC and WC/OMC, the nitrogen adsorption–desorption isotherms of the samples were recorded and shown in Fig. 5. Typical IV nitrogen adsorption/desorption isotherms with distinct hysteretic loop indicates the mesoporous structure of the as-prepared samples. The BET surface area and mesopore volume of OMC and WC/OMC are  $676\text{ m}^2\text{ g}^{-1}$  and  $0.43\text{ cm}^3\text{ g}^{-1}$ ,  $409\text{ m}^2\text{ g}^{-1}$  and  $0.47\text{ cm}^3\text{ g}^{-1}$ , respectively. The WC/OMC exhibits a high enough specific surface area to load metal particles with high dispersion. The pore size distribution, investigated by the BJH method, clearly displays a unimodal, narrow pore size distribution with a peak at about 4.3 nm for OMC and 5.0 nm for WC/OMC. Obviously, the addition of WC into OMC skeleton can expand the pore size to a certain extent, indicating its potential better electrocatalytic activity [39–43].

The electrocatalytic activity of WC/OMC was investigated by preparing its supported Pt catalysts. It can be found from TEM images (Fig. 6) that Pt nanoparticles are uniformly dispersed on the pore surface of both OMC and WC/OMC. The homogenous distribution of Pt, WC and carbon in the Pt@WC/OMC sample can be further verified through elemental mapping using SEM–EDS (Fig. 7). Moreover, the parallel arranged channels in TEM images are still kept after Pt loading process, which involves the severe conditions of the microwave process in alkaline media and acid treatment. This indicates OMC and WC/OMC possess the structure stability. From XRD results (Fig. 8), the typical diffraction peaks for Pt and WC appears, demonstrating the stability of WC in both alkaline and



**Fig. 6.** TEM images of the as-prepared Pt@OMC ((A) and (B)) and Pt@WC/OMC ((C) and (D)) catalysts.

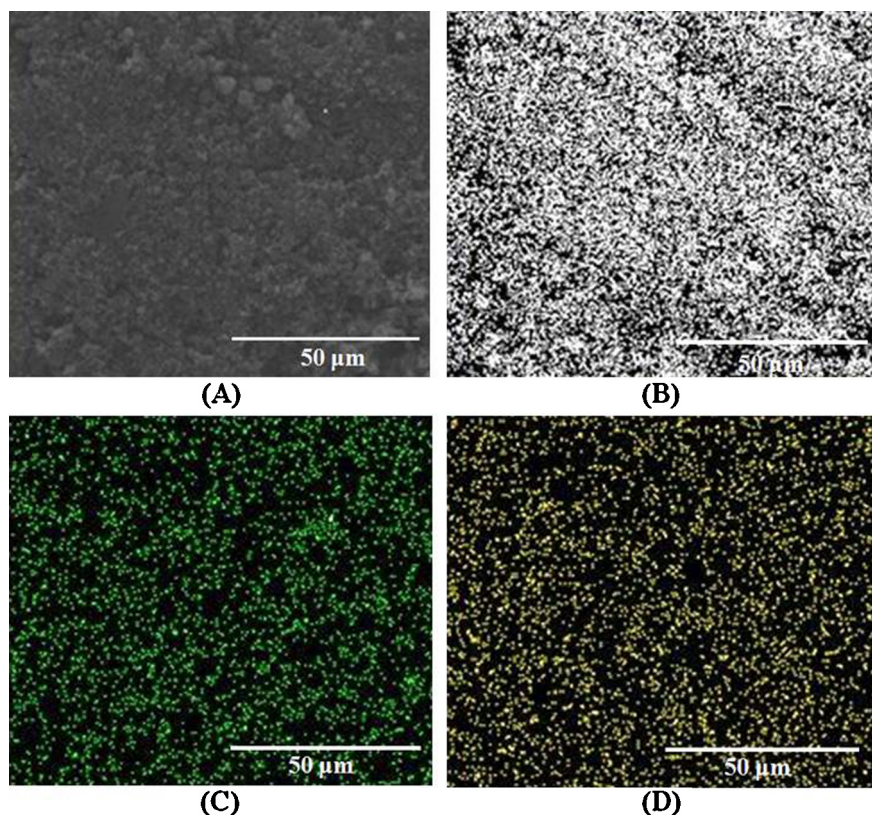


**Fig. 7.** (A) Thermal field emission environmental SEM-EDS images of the Pt@WC/OMC electrocatalyst, (B) C-elemental (C) Pt-elemental and (D) W-elemental mapping of the whole image region in (A).

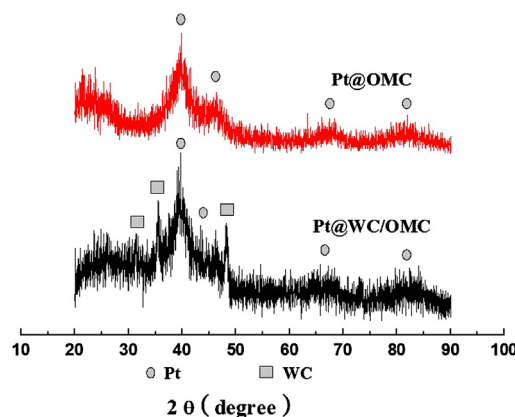


Fig. 8. XRD patterns of Pt@OMC and Pt@WC/OMC samples.

acidic environment. The low intensity of Pt peaks can be attributed to the small particle size of Pt.

Pt@WC/OMC catalysts were evaluated for methanol electrooxidation in a  $0.5 \text{ mol L}^{-1} \text{ H}_2\text{SO}_4 + 1.0 \text{ mol L}^{-1} \text{ CH}_3\text{OH}$  solution by CV technique. To further check the specific mass activity for MOR, two counterpart catalysts, Pt@OMC and the commercial PtRu@C (40 wt.% Pt, 20 wt.% Ru, Johnson Matthey Corp.), were also tested for methanol electrooxidation for comparison. The obtained CV curves (Fig. 9) exhibit very prominent characteristic peaks for methanol electrooxidation. The CV results clearly indicate that Pt@WC/OMC outperforms Pt@OMC, with a significantly

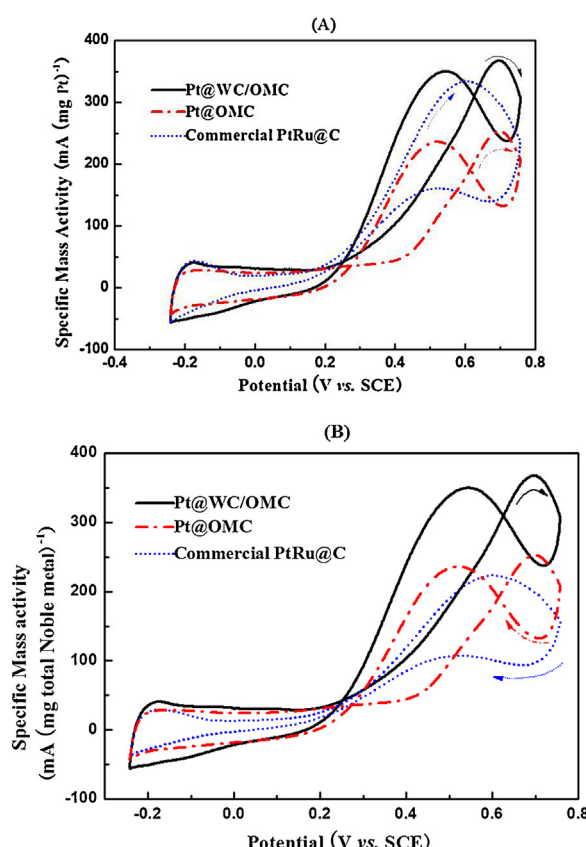


Fig. 9. Cyclic voltammograms of methanol electrooxidation at Pt@OMC, Pt@WC/OMC, and the commercial PtRu@C in  $0.5 \text{ mol L}^{-1} \text{ H}_2\text{SO}_4 + 1.0 \text{ mol L}^{-1} \text{ CH}_3\text{OH}$  solution. Scan rate:  $50 \text{ mV s}^{-1}$ .

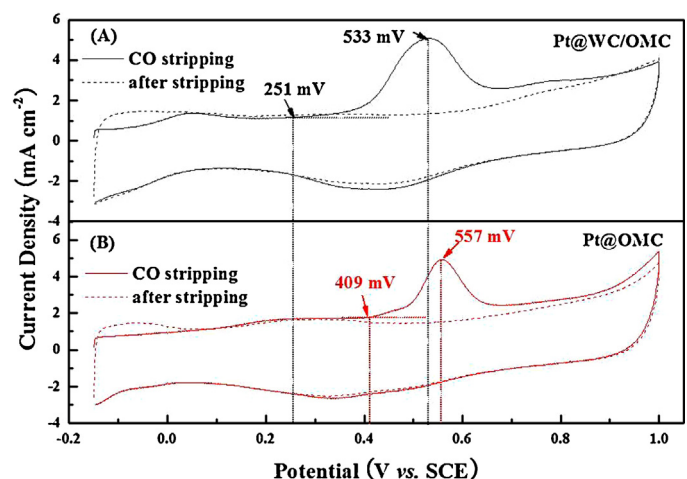
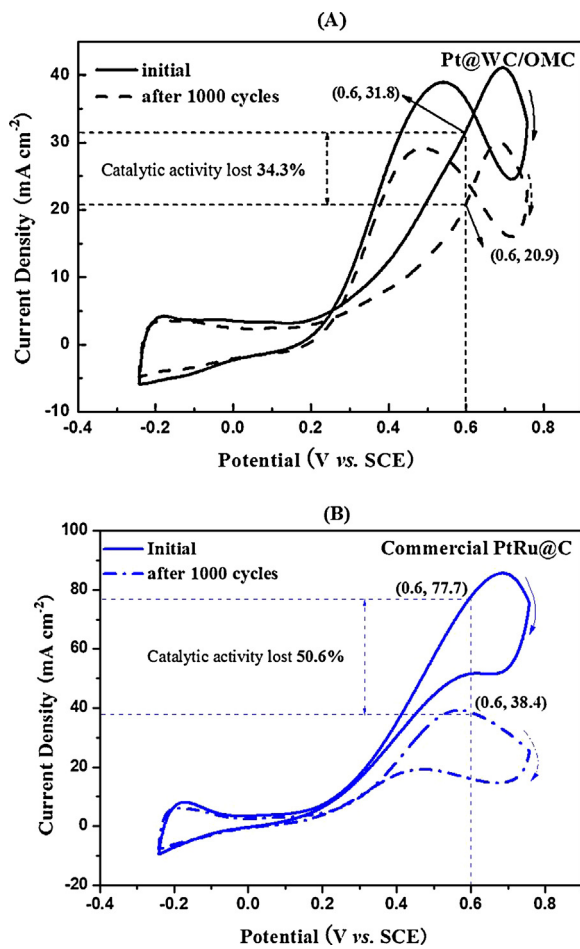


Fig. 10. CO stripping voltammetric curves at Pt@OMC and Pt@WC/OMC in  $0.5 \text{ mol L}^{-1} \text{ H}_2\text{SO}_4$  aqueous solution at a scan rate of  $20 \text{ mV s}^{-1}$ .

higher electrocatalytic peak current. The specific mass activity of Pt@WC/OMC for methanol electrooxidation is  $367.5 \text{ mA (g Pt)}^{-1}$ , which is about 1.5 times as large as that of Pt@OMC, and more encouragingly, 1.1 times the corresponding value of the commercial PtRu@C (Fig. 9 A). In addition, Ru is also a noble metal and the existence of Ru can lead to the instability of PtRu catalysts, the decreased activity of oxygen reduction reaction and the accelerated degradation of Nafion electrolyte membrane resulted from the dissolution of Ru [44–46]. The Ru-free catalyst is very attracting for the identification and development of noble-metal-economic catalysts. Considering the above issues, it is interesting to compare the specific mass activity in the unit of  $\text{mA (g total noble metal)}^{-1}$ . In this case, the specific mass activity of Pt@WC/OMC increases to 1.7 times that of the commercial PtRu@C (Fig. 9 B). This is a very important enhancement for the Pt catalyst because only adopting WC/OMC as the support material could obviously reduce the unit loading of noble metal and avoid to use Ru to achieve the same performance as the commercial PtRu@C.

The improved performance of Pt@WC/OMC could be ascribed to its highly ordered mesostructure and large surface area for high utilization efficiency of Pt and desirable mass transportation in a porous electrode [47] as well as to the synergistic effect of WC [28–31]. WC is not active to the electrooxidation of methanol and CO [28]. Its synergistic effect is reflected in the removal of the adsorbed intermediate species on Pt nanoparticles. As known, there are two steps involved in the methanol electrooxidation process, including methanol dissociative adoption on Pt to produce CO or CO-like intermediates and the further oxidation to  $\text{CO}_2$ . That is, in the process of methanol electrooxidation, the effect of WC is to promote the removal of CO or CO-like intermediates adsorbed on Pt sites to produce  $\text{CO}_2$ , and thus release the Pt active sites for further reaction. This synergistic effect of WC can also be verified by CO-stripping results (Fig. 10). The main peak potential for CO oxidation at Pt@WC/OMC is a little negative with respect to the corresponding value at Pt@OMC, whereas the onset potential of CO oxidation potential at Pt@WC/OMC is 251 mV, which is 160 mV negative than that at Pt@OMC. This demonstrates that CO or CO-like intermediates produced from methanol electrooxidation at Pt could be oxidized at a lower potential with WC/OMC as the support material, and thus improve the CO tolerance of Pt catalysts.

Durability of Pt@WC/OMC and commercial PtRu@C electrocatalyst was performed by measuring methanol electrooxidation activity before and after a continuous 1000 potential cycles by CV



**Fig. 11.** The Cyclic voltammograms of methanol electrooxidation at Pt@WC/OMC (A) and commercial PtRu@C (B) before and after 1000 potential cycles. Scanning rate:  $20 \text{ mV s}^{-1}$ .

technique. The potential cycles were between  $-0.242$  and  $0.600 \text{ V}$  at  $50 \text{ mV s}^{-1}$  in  $0.5 \text{ mol L}^{-1} \text{ H}_2\text{SO}_4 + 1.0 \text{ mol L}^{-1} \text{ CH}_3\text{OH}$  solution. The stability of the catalysts was evaluated using the anode current loss at a potential of  $0.6 \text{ V}$ . As shown in Fig. 11, the respective catalytic activity loss of Pt@WC/OMC and the commercial PtRu@C at  $0.6 \text{ V}$  is about 34% and 51%, indicating that Pt@WC/OMC is more stable than PtRu@C. The activity loss of PtRu catalyst is due to the decrease of Pt surface sites from the agglomeration of metal particles [14] and dissolution of Ru [11–14]. For Pt@WC/OMC, the activity decay could be mainly due to Pt particle size growth and Pt dissolution. The improved stability of Pt@WC/OMC could be attributed to the protection of  $\text{WO}_x$  layer in WC corrosion, which can be formed during the potential cycling and cover WC [25].

#### 4. Conclusions

In summary, an ordered mesoporous tungsten carbide/carbon composites (WC/OMC) with high specific surface area was successfully synthesized by combining a hydrothermal reaction and a hard template method with ordered mesoporous silica SBA-15 as a hard template. Pt supported on WC/OMC electrocatalyst exhibited higher specific mass activity for methanol electrooxidation, and proved to be more stable than the commercial PtRu@C electrocatalyst and high CO tolerance than the Pt@OMC electrocatalyst. These significant improvements are of vital importance for the identification and development of low noble-metal catalysts for DMFCs applications. Finally it is worth to be noticed that the present work could also render a universal approach for the preparation of other

ordered mesoporous composite materials for various important applications.

#### Acknowledgments

The authors would like to thank the financial support of the National Natural Science Foundation of China (Grant No. 21276290 and 21107145) and the “Sino-Greek Science and Technology Cooperation Project (2013DFG62590)” for funding. We also thank the research fund of the Key Laboratory of Fuel Cell Technology of Guangdong Province and Undergraduate Program for Physics Base from School of Physics and Engineering, Sun Yat-sen University.

#### References

- [1] [http://www.viaspace.com/ae\\_dmfc.php](http://www.viaspace.com/ae_dmfc.php)
- [2] R. Bashyam, P. Zelenay, *Nature* 443 (2006) 63–66.
- [3] M. Soszko, M. Łukaszewski, Z. Mianowska, A. Czerwiński, *J. Power Sources* 196 (2011) 3513–3522.
- [4] E.C. Weiger, M.B. Zellner, A.L. Stottlmyer, J.G.G. Chen, *Top. Catal.* 46 (2007) 349–357.
- [5] X. Li, J. Liu, Q. Huang, W. Vogel, D.L. Akins, H. Yang, *Electrochim. Acta* 56 (2001) 278–284.
- [6] S. Garbarino, A. Ponrouch, S. Pronovost, D. Guay, *Electrochim. Commun.* 11 (2009) 1449–1452.
- [7] K.S. Lee, S.J. Yoo, J.H. Jang, Y.E. Sung, *Electrochim. Acta* 56 (2011) 8688–8694.
- [8] J.G. Liu, Z.H. Zhou, X.X. Zhao, Q. Xin, G.Q. Sun, B.L. Yi, *Phys. Chem. Chem. Phys.* 6 (2004) 134–137.
- [9] W. Wang, Y. Li, H. Wang, *Micro Nano Lett.* 8 (2013) 23–26.
- [10] Z.X. Liang, T.S. Zhao, J.B. Xu, *J. Power Sources* 185 (2008) 166–170.
- [11] C.Z. He, H.R. Kunz, J.M. Fenton, *J. Electrochim. Soc.* 144 (1997) 970–979.
- [12] T.I. Valdez, S. Firdosy, B.E. Koel, S.R. Narayanan, *ECS Trans.* 1 (2006) 293–303.
- [13] P. Piela, C. Eickes, E. Brosha, F. Garzon, P. Zelenay, *J. Electrochim. Soc.* 151 (2004) A2053–A2059.
- [14] W.M. Chen, G.Q. Sun, J.S. Guo, X.S. Zhao, S.Y. Yan, J. Tian, S.H. Tang, Z.H. Zhou, Q. Xin, *Electrochim. Acta* 51 (2006) 2391–2399.
- [15] R. Simon, R. Vallance, S. Kingman, D.H. Gregory, *Adv. Mater.* 19 (2007) 138–142.
- [16] L. Bartha, P. Atato, L.A. Toth, R. Porat, S. Berger, A. Rosen, *Adv. Mater.* 32 (2000) 23–26.
- [17] R.L. Levy, M. Boudart, *Science* 181 (1973) 547–549.
- [18] N. Ji, T. Zhang, M.Y. Zheng, A.Q. Wang, H. Wang, X.D. Wang, J.G.G. Chen, *Angew. Chem. Int. Ed.* 120 (2008) 8638–8641.
- [19] S. Bodardo, M. Maja, N. Penazzi, F.E.G. Henn, *Electrochim. Acta* 42 (1997) 2603–2609.
- [20] C.J. Barnett, G.T. Burstein, A.R.J. Kucernak, K.R. Williams, *Electrochim. Acta* 42 (1997) 2381–2388.
- [21] H. Chihna, S. Campbell, O. Kesler, *J. Power Sources* 164 (2007) 431–440.
- [22] M.B. Zellner, J.G.G. Chen, *Catal. Today* 99 (2005) 299–307.
- [23] A. Serov, C. Kwak, *Appl. Catal. B: Environ.* 90 (2009) 313–320.
- [24] E.C. Weigert, D.V. Esposito, J.G.G. Chen, *J. Power Sources* 193 (2009) 501–506.
- [25] M. Shao, B. Merzougui, K. Shoemaker, L. Stolar, L. Protsailo, Z.J. Mellinger, I.J. Hsu, J.G.G. Chen, *J. Power Sources* 196 (2011) 7426–7434.
- [26] J.B. Christian, S.P.E. Smith, M.S. Whittingham, H.D. Abruua, *Electrochim. Commun.* 9 (2007) 2128–2132.
- [27] M.K. Jeon, H. Daimon, K.R. Lee, A. Nakahara, S.I. Woo, *Electrochim. Commun.* 9 (2007) 2692–2695.
- [28] Y. Wang, S.Q. Song, P.K. Shen, C.X. Guo, C.M. Li, *J. Mater. Chem.* 19 (2009) 6149–6153.
- [29] R. Ganesan, J.S. Lee, *Angew. Chem. Int. Ed.* 44 (2005) 6557–6560.
- [30] Y. Wang, C. He, A. Brouzgou, Y. Liang, R. Fu, D. Wu, P. Tsakarais, S. Song, *J. Power Sources* 200 (2012) 8–13.
- [31] P.K. Shen, S. Yin, Z. Li, C. Chen, *Electrochim. Acta* 55 (2010) 7969–7974.
- [32] J.S. Beck, C.T.W. Chu, I.D. Johnson, C.T. Kresge, M.E. Leonowicz, W.J. Roth, J.W. Vartuli, *WO Patent* 91/11390, 1991.
- [33] A. Taguchi, F. Schütt, *Micropor. Mesopor. Mater.* 77 (2005) 1–45.
- [34] Z. Wu, Y. Yang, D. Gu, Q. Li, D. Feng, Z. Chen, B. Tu, P.A. Webley, D. Zhao, *Small* 5 (2009) 2738–2749.
- [35] R. Ryoo, S.H. Joo, M. Kruk, M. Jaroniec, *Adv. Mater.* 13 (2001) 677–681.
- [36] S. Song, Y. Wang, P.K. Shen, *J. Power Sources* 170 (2007) 46–49.
- [37] S. Song, J. Liu, J. Shi, H. Liu, V. Maragou, Y. Wang, P. Tsakarais, *Appl. Catal. B* 103 (2011) 287–293.
- [38] Y. Meng, D. Gu, F.Q. Zhang, Y.F. Shi, H.F. Yang, Z. Li, C.Z. Yu, B. Tu, D.Y. Zhao, *Angew. Chem. Int. Ed.* 44 (2005) 7053–7059.
- [39] S. Song, S. Yin, Z. Li, P.K. Shen, R. Fu, D. Wu, *J. Power Sources* 195 (2010) 1946–1949.
- [40] G.S. Chai, S.B. Yoon, J.S. Yu, J.H. Choi, Y.E. Sung, *J. Phys. Chem. B* 108 (2004) 7074–7079.
- [41] S.H. Joo, H.I. Lee, D.J. You, K. Kwon, J.H. Kim, Y.S. Choi, M. Kang, J.M. Kim, C. Pak, H. Chang, D. Seung, *Carbon* 46 (2008) 2034–2045.

- [42] J. Marie, R. Chenitz, M. Chatenet, S. Berthon-Fabry, N. Cornet, P. Achard, *J. Power Sources* 190 (2009) 423–434.
- [43] H.D. Du, L. Gan, B.H. Li, P. Wu, Y.L. Qiu, F.Y. Kang, Y.Q. Zeng, *J. Phys. Chem. C* 111 (2007) 2040–2043.
- [44] S. Kang, S. Lim, D.H. Peck, S.K. Kim, D.H. Jung, S.H. Hong, H.G. Jung, Y. Shul, *Int. J. Hydrogen Energy* 37 (2012) 4685–4693.
- [45] W.B. Wang, X.P. Wang, P.J. Zuo, B.Q. Yang, G.P. Yin, X.P. Feng, *J. Power Sources* 181 (2008) 93–100.
- [46] L. Subramanyam Sarma, C.H. Chen, G.R. Wang, K.L. Hsueh, C.P. Huang, H.S. Sheu, D.G. Liu, J.F. Lee, B.J. Hwang, *J. Power Sources* 167 (2007) 358–365.
- [47] C.X. He, Y.R. Liang, R.W. Fu, D.C. Wu, S.Q. Song, R. Cai, *J. Mater. Chem.* 21 (2011) 16357–16364.